EVOLUTION OF THE ELECTRON TEMPERATURE PROFILE OF OHMICALLY HEATED PLASMAS IN TFTR

G. Taylor, P.C. Efthimion, V. Arunasalam, R.J. Goldston, B. Grek
K.W. Hill, D.W. Johnson, K. McGuire, A.T. Ramsey, and F.J. Stauffer

Princeton University
Princeton Plasma Physics Laboratory
Princeton, NJ 08544

PPPL--2221
DE85 017687

ABSTRACT

Blackbody electron cyclotron emission was used to ascertain and study the evolution and behavior of the electron temperature profile in ohmically heated plasmas in the Tokamak Fusion Test Reactor (TFTR). The emission was measured with absolutely calibrated millimeter wavelength radiometers. The temperature profile normalized to the central temperature and minor radius is observed to broaden substantially with decreasing limiter safety factor q_a, and is insensitive to the plasma minor radius. Sawtooth activity was seen in the core of most TFTR discharges and appeared to be associated with a flattening of the electron temperature profile within the plasma core where $q \leq 1$. Two types of sawtooth behavior were identified in large TFTR plasmas (minor radius, $a \geq 0.8$ m) : a typically 35 - 40 msec period "normal" sawtooth, and a "compound" sawtooth with 70 - 80 msec period. The compound sawtooth was characterized by what appeared to be a partial reconnection, which occurs away from the plasma core, in addition to a full reconnection. A multiple linear regression analysis of the central electron temperature [$T_e(o)$] with toroidal field (B_T), major radius (R), minor radius (a), plasma current (I_p) and

effective ion charge (Z_{eff}) results in a scaling of the form, $T_e(o) \propto B_T^{0.78} R^{-0.31} a^{1.1} Z_{eff}^{0.45} I_p^{-0.24}$, where the major radial dependence was obtained by comparison with earlier PLT data. This temperature scaling is consistent with the TFTR confinement scaling of Efthimion *et al.* [1].

1. INTRODUCTION

Past studies of tokamak plasmas have shown an improvement of plasma confinement with plasma size. The present generation of large tokamaks (TFTR, JET, JT60, T15) will determine the extent to which this trend will continue. Central to the study of plasma confinement and transport is the measurement of the electron temperature profile. We present here a detailed study of the temporal evolution of the electron temperature profile of ohmically heated plasmas in the Tokamak Fusion Test Reactor (TFTR). Electron temperature profiles ascertained from the electron cyclotron emission have been utilized in the initial confinement studies of ohmically heated plasmas in TFTR [1-3].

Plasmas were studied in TFTR with minor radii (a) of 0.83, 0.69, 0.55, 0.41 m and major radii (R) in the range of 2.55 - 2.70 m. The largest minor radius plasmas had currents in the range of I_p = 0.6 - 2.2 MA with a toroidal field (B_T) up to 4.8 T and a line average density in the range of $\bar{n}_e$ = 0.8 - 5 x $10^{19} m^{-3}$.

In this paper the electron temperature profile was ascertained by measuring the intensity of the electron cyclotron emission. It is well-known that in dense high-temperature plasmas the intensity of the electron cyclotron emission for the fundamental ($\omega = \Omega_{ce}$) ordinary mode and second harmonic ($\omega = 2\Omega_{ce}$) extraordinary mode is at the blackbody level [4-8]. Since the magnetic field varies approximately inversely with the major radius in a tokamak, the emission frequency is localized in position. Fast frequency scanning heterodyne receivers [7,9] allow the study of electron temperature as a function of both time and major radius within a single discharge. Because of the longer plasma time scales in the larger tokamaks and the improvements in technology which have led to shorter scan times of heterodyne receivers, electron cyclotron emission provides excellent time-resolved measurements of temperature profiles for detailed study of sawtooth effects.

A brief description of the TFTR fast scanning cyclotron receivers is presented in section 2 of this paper. Included is a discussion of the instrumental resolution and the resulting accuracy of measurements. Section 3 presents electron temperature profile data which includes a summary of the evolution of the profile during a plasma discharge and the dependence of the temperature profile on the limiter safety factor (q_a), $\bar{n}_e$ and a. A comparison of the electron temperature profile measured with the radiometer and TV Thomson scattering is also shown. Profile evolution during electron temperature sawtooth fluctuations and its implications for the shape of the current density profile are discussed in section 4. Then we investigate the scaling of the central electron temperature in section 5 and compare the data from TFTR and earlier data from PLT with the semi-empirical central temperature scalings of Perkins [10] and Tang et al. [11]. We also discuss its implications for confinement time scaling. Conclusions and future plans are stated in section 6. Many of the features of the electron temperature profile of ohmically heated plasmas in TFTR have been observed in other tokamaks. However, the central temperature scaling and the electron temperature profile evolution in compound sawtooth ohmic discharges have not been reported in the literature.

2. EXPERIMENTAL ARRANGEMENT

A simplified schematic of the TFTR cyclotron radiometers is shown in Fig. 1. The instruments were absolutely calibrated, in situ, using a Dicke [12] switching integration technique to an accuracy of better than 10% [13] with room temperature and liquid nitrogen cooled blackbody sources. Details of the receivers have been discussed elsewhere [9]. The transmission system between TFTR and the receivers was designed to operate between 75 GHz and

210 GHz. This spectral range required three scanning millimeter wavelength receivers, each covering a different region of the transmission system bandwidth. Power splitters direct cyclotron radiation to each of the receivers which are located in the diagnostic basement under TFTR. The receivers can be independently swept through their full operational frequency range in 2 msec every 4 msec. This capability allows an electron temperature profile to be determined every 4 msec. The receivers can also be individually tuned remotely to dwell at one frequency to allow the study of fast temperature fluctuations at one plasma position with a time resolution of less than 100 μsec. The major radial resolution (3 - 5 cm) of the receivers is determined by their bandwidths and is somewhat larger than the thickness of the cyclotron resonance layer. The spatial resolution in the toroidal and vertical directions at 75 GHz is limited to 15 - 20 cm at the center of the TFTR vacuum vessel by diffraction from optical components in the transmission system. At 170 GHz, diffraction is significantly less, and the spatial resolution is better than 10 cm. Plasma refraction effects are negligible compared to the optical resolution limits at the line average electron densities $\bar{n}_e \leq 5 \times 10^{19} m^{-3}$ studied here.

The measurements presented in sections 3-5 were made with only two receivers, operating at 75-110 GHz and 110-170 GHz respectively with toroidal fields (B_T) up to 4.8 T. The cyclotron emission was measured at both the fundamental ($\omega = \Omega_{ce}$) ordinary mode, and second harmonic ($\omega = 2\Omega_{ce}$) extraordinary mode. The emission intensity I_ω received by the radiometer antenna is given by

$$I_\omega = \kappa T_e \Delta f \ (1-e^{-\tau}) \ , \qquad (1)$$

where Δf is the bandwidth of the receiver, τ is the optical depth, and κ is Boltzmann's constant [8]. In a plasma with a Maxwellian electron velocity

distribution (i.e. when runaway electrons are insignificant), $\tau \geq 2$ is sufficient to produce a blackbody emission intensity level, and the electron temperature is the only plasma parameter that determines the emission intensity. For the second harmonic extraordinary mode, the optical depth is given by

$$\tau_{ex}(\omega = 2\Omega_{ce}) = 2\beta\left\{\frac{6\Omega_{ce}^2 - \omega_{pe}^2}{6\Omega_{ce}^2 - 2\omega_{pe}^2}\right\}^2 \left(1 - \frac{\omega_{pe}^2}{4\Omega_{ce}^2}\right)^{1/2}, \qquad (2)$$

where $\beta = \frac{R\pi\omega_{pe}^2 \kappa T_e}{2\Omega_{ce} mc^3}$, ω_{pe} is the electron plasma frequency, Ω_{ce} is the electron cyclotron frequency, m is the electron mass, and c is the velocity of light. For the first harmonic ordinary mode, the optical depth is

$$\tau_{or}(\omega = \Omega_{ce}) = \beta\left(1 - \frac{\omega_{pe}^2}{\Omega_{ce}^2}\right)^{1/2}. \qquad (3)$$

$\tau_{or}(\omega = \Omega_{ce}) \geq 7$ and $\tau_{ex}(\omega = 2\Omega_{ce}) \geq 20$ in the center of a TFTR discharge with $B_T = 2.7T$, $T_{eo} = 2$ keV and $\bar{n}_e = 3 \times 10^{19} m^{-3}$.

Since Ω_{ce} depends on B, an accurate determination of B(R) is required to obtain good radial profiles of T_e. At a minor radial position r and for small (r/R) the magnitude of the total field variation δB from the 1/R dependent toroidal field B_o is given by [14]

$$\frac{\delta B}{B_o} = \frac{\bar{B}}{B_o} + \tfrac{1}{2} b_\theta^2, \qquad (4)$$

where $b_\theta(r)$ is the normalized poloidal field defined by

$$b_\theta(r) = \frac{\mu_o}{B_o} \frac{\int_0^r j(r')r'dr'}{r}, \qquad (5)$$

$j(r)$ is the current density, and u_o is the permeability of free space. Here $\tilde{B}(r)$ is the paramagnetic contribution given by

$$-\frac{1}{B_o}\frac{d\tilde{B}}{dr} = \frac{1}{2}\left\{\frac{d\beta_\perp}{dr} + \frac{db_\theta^2}{dr}\right\} + \frac{b_\theta^2}{r}, \qquad (6)$$

where $\beta_\perp$ is the normalized perpendicular plasma pressure. The local poloidal component of the magnetic field and plasma paramagnetic effects contributed to a 1 - 4% variation in the total magnetic field from an inverse major radial dependence. For the data presented here, both these effects resulted in a total variation of 0.03 to 0.1 m in the position measurements deduced from a simple inverse, major radial field dependence (i.e., in the mapping of the emission frequency to the major radial position). These effects were included in all the figures except for Fig. 3.

3. ELECTRON TEMPERATURE PROFILE BEHAVIOR

The evolution of plasma current (I_p), line integral density ($\bar{n}_e\ell$), and the surface voltage (V_S) in a TFTR discharge with 0.83 m minor radius, a plasma current of 1.4 MA, and a toroidal field of 2.7 T is shown in Fig. 2. I_p rises to a constant value of 1.4 MA in approximately 1.7 seconds. V_S falls throughout the current flattop, and $\bar{n}_e\ell$ reaches a steady value of $5 \times 10^{19} m^{-2}$ at the beginning of the current flattop. The electron temperature profile [$T_e(R)$] evolution for this discharge is summarized in Fig. 3. In this figure the major radial position does not include poloidal field and paramagnetic effects in the frequency to position mapping. During the first second of the pulse $T_e(R)$ becomes increasingly peaked, with a maximum central temperature over 2 keV. The profile then broadens; the central temperature falls rapidly to 1.7 keV and it remains at this level until the end of the current

flattop. As the profile broadens, temperature sawtooth fluctuations appear in the center of the plasma. Sawteeth will be discussed in more detail in Section 4. The profiles shown in Fig. 3 and the other figures discussed in this section were averaged over 100 msec to remove fluctuations in the profile due to sawteeth. Figure 4 illustrates the agreement between the radiometer profiles and the corresponding ones obtained from a multichannel TV Thomson scattering system [15] at the same time during the flattop of a 1.4 MA discharge. This agreement was obtained only after the radiometer profiles were analyzed with paramagnetic and poloidal field effects included in the mapping of the emission frequency to the major radial position.

Temperature profile broadening during the current flattop was found to be more significant for discharges with lower limiter safety factors (q_a), as illustrated in Fig. 5. These temperature profiles are for discharges with different currents from 800 kA to 1.5 MA at B_T = 2.7 T corresponding to a change in q_a from 4.7 to 2.5. These discharges had line average electron densities, $\bar{n}_e$ = 2.1 - 2.3 x $10^{19} m^{-3}$. The arrows in this figure indicate the position of the q = 1 surface for each profile. The radius of the q = 1 surface increased with decreasing q_a, while the central temperature remained relatively constant. The temperature within 15 cm of the limiter increased significantly with decreasing q_a. This increased edge temperature correlated with an increase in the metallic impurity content of the plasma, measured by an x-ray pulse height analyzer [1]. The profile shapes appear to depend on q_a in agreement with the principle of profile consistency [16,17]; this essentially implies that the ratio of the central electron temperature to the average temperature is only a function of q_a. In addition the central temperature decreased with increasing $\bar{n}_e$. This density dependence, illustrated in Fig. 6 for q_a = 3, and 0.83 m minor radius plasmas is

associated with an inverse dependence of Z_{eff} on $\bar{n}_e$ [2], as will be shown in section 5.

Fig. 7 summarizes the behavior of the temperature profile for plasmas with $q_a \approx 3$ and minor radii of a = 0.55m, 0.69 m and 0.83m, and $\bar{n}_e$ in the range 2.3 - 2.6 x $10^{19} m^{-3}$. The profile shape appears to be independent of the plasma minor radius and is determined by q_a. Indeed, from Fig. 5 and 7, $r_1/a \sim 1/q_a$, where r_1 is the minor radius of the q = 1 surface. Experimentally we observe a significant temperature gradient outside the sawtooth inversion surface. This appears to be a region of low thermal conductivity and effective thermal confinement, while inside the sawtooth inversion surface is a region of effective thermal conductivity.

4. ELECTRON TEMPERATURE SAWTOOTH FLUCTUATIONS

For almost all of the a $\gtrsim$ 0.8 m TFTR discharges the time evolution of the central electron temperature shows well-defined, large amplitude sawtooth fluctuations [18-20]. Figure 8 shows the evolution of the central temperature for the $q_a \approx 3$ discharge shown in Figs. 2 and 3. The filled circles show the central electron temperature measurements from an X-ray pulse height analyzer with an averaging time of 100 msec [1]. The maximum central electron temperature is attained at 1 s. Simultaneous with the fall of the electron temperature at this time is the development of 30 - 40 msec period sawtooth fluctuations. Later in the discharge the central temperature exhibits sawteeth with almost twice the amplitude and period of the initial sawteeth. These latter sawteeth will be referred to as "compound" sawteeth and the former short period fluctuations as "normal" sawteeth.

The evolution of the temperature profile during compound sawteeth in the current flattop region of a $q_a \approx 3$ discharge is shown in Fig. 9. These

sawteeth dominate the plasma core within 0.35 m of the magnetic axis which is located at 2.6 m major radius. Inverted sawteeth can be readily observed out to 0.7 m from the magnetic axis, which is only 0.1 - 0.15 m from the limiter.

The profile evolution is different for normal and compound sawteeth. Examples of each of these are shown in Figures 10 and 11, respectively. *During the rise of a normal sawtooth* the profile grows slightly peaked, and when the sawtooth relaxes, the profile appears to become hollowed. However, the accuracy of our measurements (± 10%) are insufficient to discount it from being flat. During the ramp-up of compound sawteeth, an exchange of hotter core plasma with plasma further from the plasma axis occurs as illustrated by profiles A and B in Fig. 11. This exchange occurs, 0.2 - 0.4 m from the axis of the plasma, so that the central temperature continues to increase. Eventually the profile (Profile C) becomes more peaked than in the case of normal sawteeth and subsequently relaxes (Profile D) to a hollow profile this relaxation includes plasma across the whole of the core region.

The observed evolution of the temperature profile during compound sawteeth is consistent with the existence of a hollow current density profile with two $q \approx 1$ surfaces [21,22]. During the current flattop the sawtooth behavior often makes several transitions between normal and compound activity. Discharges with the same $\bar{n}_e$ and q_a exhibit varying degrees of this compound activity, although compound sawteeth are more commonly seen at lower values of q_a [23]. It is possible that the current density profile is therefore also hollow during the normal sawtooth, but that the hollowness is insufficient to produce conditions necessary for the partial reconnection to occur. This transition has been considered in more detail by Parail and Pereverzev [24].

Discharges dominated by compound sawteeth appeared to have essentially the same global energy confinement as those containing predominantly normal

sawteeth. In both cases the presence of the sawteeth may be associated with the flattening of the time averaged $T_e(R)$ profiles in the plasma core in low q_a discharges. The minor radial mixing which occurs at the onset of sawtooth activity could result in a significant reduction in the peak electron temperature which can be obtained during the current flattop. The sawtooth fluctuation period (τ_s) was compared to the growth time of the m = 1 resistive tearing mode. In particular we compared τ_s to the analytical prediction of *McGuire and Robinson [25], namely,*

$$\tau_s \sim 3\tau_R^{3/7}\tau_A^{2/7}\tau_h^{2/7}, \qquad (7)$$

where $\tau_R = r_1^2/\eta$ is the resistive diffusion time, $\tau_A = Rp^{1/2}/B_T$ is the Alfven transit time, $\tau_h = 3nT_e/2\eta j^2$ is the heating time, ρ is the mass density, η is the resistivity, j is the central current density, and r_1 is the sawtooth inversion radius. The McGuire-Robinson model assumes that the resistive mode heating is terminated when the m = 1 island grows to r_1 and it does not *include diamagnetic drift effects.* We found that the compound sawteeth agreed well with this scaling, but that the normal sawteeth seen in large TFTR plasmas did not. Yamada et al. [26] have come to a similar conclusion after analyzing data from an X-ray imaging system for a large number of TFTR discharges, including plasmas with $0.41\ m \leq a \leq 0.83\ m$. In addition, they find that the period of sawteeth seen in smaller TFTR discharges, $a \leq 0.6$ m, also agrees with the McGuire and Robinson scaling.

5. CENTRAL ELECTRON TEMPERATURE SCALING

In the light of studies [27] which propose a fusion reactor scenario where the plasma is brought to ignition primarily by ohmic heating, the

central temperature scaling in ohmic plasmas takes on a new significance.

Perkins [10] and Tang et al. [11] have recently developed semi-empirical models which are based on the observation that there is effective thermal confinement in the $1 \leq q \leq 2$ region of the plasma profile. They assume that heat transport in this region is driven by a drift wave mechanism and that the radial dependence of T_e is determined by profile consistency [16]. Perkins model constrains the electron temperature profile to zero at the $q = 2$ surface and the electron density profile is assumed to be a gaussian. In contrast Tang et al. assume a gaussian temperature profile in which $r_1/a = 1/q_a$ and a parabolic density profile. The formalism of the two heat transport models also differs in that Perkins takes a somewhat heuristic approach in which the drift wave growth rate is governed by a diamagnetic drift frequency which is sensitive to density gradients where as Tang et al. use a self-consistent theory where the drift wave growth rate is sensitive to density and temperature gradients. Both these models have been used to derive the effective thermal diffusivity due to drift wave turbulence and through the heat balance equation,

$$\frac{1}{r}\frac{d}{dr}\left(n_e r\, \chi_e(r)\right)\frac{d\,T_e(r)}{dr} = P_{OH} \quad , \tag{8}$$

where P_{OH} is the ohmic input power, a parametric dependence for $T_e(o)$ has been derived. Both these models assume transport due to radiation, convection and charge exchange is insignificant in the $1 \leq q \leq 2$ region. The $T_e(o)$ scaling of Tang et al. [11] is

$$T_e(o) \sim B_T^{0.5} R^{0.1} Z_{eff}^{0.3} I_p^{0.2}, \tag{9}$$

and Perkins [10] is

$$T_e(o) \sim B_T^{0.8} R^{-0.2} a^{0.66} Z_{eff}^{0.33} I_p^{-0.12} \tag{10}$$

Both models predict a strong dependence of $T_e(o)$ on B_T and a somewhat weaker dependence on Z_{eff}. They also predict that $T_e(o)$ is independent of $\bar{n}_e$ at fixed Z_{eff}. Data presented in Section 3 showed that $T_e(o)$ *decreased with* increasing $\bar{n}_e$ in TFTR but further study of this dependence indicates that this is the result of the density dependence of Z_{eff}. In fig. 12 we illustrate this interpretation for two density scans taken at I_p = 1.8 MA, B_T = 4T. One density scan was taken 6 weeks after the other so that although the scans were over a similar density range the Z_{eff} was lower at fixed density for the later scan, due to TFTR having become somewhat cleaner. Fig. 12(a) shows the Z_{eff} from visible bremsstrahlung as a function of $\bar{n}_e$ for the two scans and fig. 12(b) shows $T_e(o)/Z_{eff}^{0.5}$ plotted against $\bar{n}_e$. If $T_e(o)$ is independent of $\bar{n}_e$ and dependent on $Z_{eff}^{0.5}$ we would expect the data from the two density scans to fall on the same horizontal line in fig. 12(b) which indeed they do.

To determine a $T_e(o)$ scaling for TFTR, a multiple linear regression analysis was applied to the TFTR data set and to data obtained from PLT. In order to determine the $T_e(o)$ dependence on B_T, a, Z_{eff}, and I_p a TFTR dataset was used with deuterium, hydrogen and helium discharges having $1.8 \leq B_T \leq 4.8$ T, $0.41 \leq a \leq 0.83$m, neoclassical Z_{eff} between 1.6 and 5.2, and $0.27 \leq I_p \leq 2.2$ MA. Data from a scanning Michelson interferometer [28] was used to obtain temperature data for the TFTR a = 0.41 m discharges. The R dependence was found by including deuterium and hydrogen PLT data where R = 1.32 m, a = 0.4 m, and B_T = 3.2 T. Essentially the data from over 200 plasma discharges were used in the regression analysis. The PLT data includes neon discharges with Z_{eff} ~ 8 [29]. A $T_e(o)$ empirical scaling of the form:

$$T_e(o) \propto B_T^{0.78 \pm 0.07} R^{-0.31 \pm 0.06} a^{1.1 \pm 0.1} Z_{eff}^{0.45 \pm 0.05} I_p^{-0.24 \pm 0.06} \tag{11}$$

was found. $\bar{n}_e$ was not included as an independent variable in regression since we found $T_e(o)$ to be independent of $\bar{n}_e$ at fixed Z_{eff}. Figure 13 is a plot of the central temperature against the empirical scaling. The TFTR data includes B_T = 2.7 T (squares), 4 T (stars), 4.8 T (diamonds) deuterium, hydrogen and helium discharges with .5 < a < .83 m. Also plotted are TFTR a = 0.41 m deuterium discharges (triangles) where the central temperature was obtained using a scanning Michelson interferometer [28]. The PLT hydrogen and deuterium discharges (shown by crosses) include both carbon and stainless steel limiters. The datasets do not include shots where confinement seemed to saturate with density and where ion transport was dominant according to power balance calculations. The neoclassical value was used for Z_{eff} in this study. On TFTR the impurity Z_{eff} measurements tend to lie between the estimates obtained from the Spitzer and neoclassical resistivity models. A regression on TFTR data where visible bremsstrahlung data was available yielded a similar dependence of Z_{eff} as that obtained when using the neoclassical Z_{eff}. The TFTR temperature scaling is significantly different to that obtained by Pfeiffer and Waltz [30], however, earlier work by Gondhalekar et al. [31] on Alcator shows a strong toroidal field dependence similar to that seen on TFTR.

Adopting the technique in Perkins [10] and Tang et al. [11], the central electron temperature can be related to the total energy confinement through the energy balance equation for ohmic heating. Assuming the electron density profile is parabolic and the electron temperature profile is gaussian in shape and obeys profile consistency, then

$$T_e(r) = T_e(o)\exp\left(- \frac{2}{3} \alpha_n \frac{r^2}{a^2} \right) \qquad (12)$$

where $\alpha_n = (q_a + 0.5)$. Assuming $T_e = T_i$ and that the plasma has an atomic number $Z = 1$ and a generic impurity with $Z = 10$ the ion number density $n_i = n_e(1.1 - 0.1\, Z_{eff})$. Therefore, the confinement time, τ_E is given by:

$$\tau_E \propto \frac{R(2.1 - 0.1\, Z_{eff}) \int_o^a n_e(r)\, T_e(r)\, rdr}{R \int_o^a nJ(r)^2\, rdr} , \qquad (13)$$

where $j(o) \propto B_T^2/R^2$ and $n \propto Z_{eff}/T_e^{3/2}$.

After integration, (13) becomes:

$$\tau_E \propto \frac{R^2\, \bar{n}_e\, T_e(o)^{5/2} q_a^{0.3} (2.1 - 0.1\, Z_{eff})}{Z_{eff}\, B_T^2} \qquad (14)$$

Note that the confinement time in (14) is a very strong function of the central temperature and any uncertainties in the parametric dependence of $T_e(o)$ will greatly increase the uncertainties in τ_E. However, the relation in (14) has some interesting implications; since $T_e(o)$ from the regression analysis is insensitive to density, it follows from substitution of (11) in (14) that the confinement time increases linearly with $\bar{n}_e$. Similarly one would conclude that τ_E is insensitive to Z_{eff} and that the confinement is a strong function of both minor and major radius.

Indeed it is also possible to determine a temperature scaling from (14) by substituting the TFTR confinement scaling of Efthimion et al. [1], namely:

$$\tau_E \propto \bar{n}_e R^2 a q_a \qquad (15)$$

This leads to a $T_e(o)$ parametric dependence of the form:

$$T_e(o) \propto B^{1.08}R^{-0.28}a^{0.96}\left(\frac{Z_{eff}}{2.1 - 0.1\,Z_{eff}}\right)^{0.4} I_p^{-0.28} \quad . \qquad (16)$$

This expression is very similar to the dependence obtained in (11).

6. CONCLUSIONS AND FUTURE WORK

Fast scanning cyclotron radiometers operating between 75 and 170 GHz, and absolutely calibrated in situ, have been used successfully to study the time evolution of the electron temperature profiles in TFTR ohmic discharges in sufficient detail to study the temperature sawtooth in the plasma core. Such measurements are essential for plasma confinement and transport studies [1,2]. $T_e(R)$ is observed to broaden with decreasing q_a, and the normalized profile shape is found to be insensitive to variations in minor radius. These observations support the principle of profile consistency [16,17]. Compound sawteeth which involve a partial reconnection away from the plasma core as well as a full reconnection are often seen in TFTR discharges. Their temperature profile behavior is consistent with the existence of two $q = 1$ surfaces and a significant hollowing of the current density profile [21,22]. A regression analysis of $T_e(o)$ yields an empirical dependence of the form:

$$T_e(o) \sim B_T^{0.78}R^{-0.31}a^{1.1}Z_{eff}^{0.45}I_p^{-.24},$$

and when the Z_{eff} dependence is removed $T_e(o)$ is found to be independent of $\bar{n}_e$. The central temperature scaling appears to be consistent with the TFTR confinement scaling [1].

Recently, experiments on TFTR have been extended to $B_T = 5.2$T and plasma currents of up to 2.5 MA. The addition of a 170-210 GHz radiometer will allow a study of temperature scaling at $B_T \geq 5$ T and currents ≥ 3.0 MA.

ACKNOWLEDGEMENT

We would like to thank H.P. Furth, L.C. Johnson, D. M. Meade, F. Perkins, N.R. Sauthoff, J.F. Schivell, S. Sesnic, W. Tang, and K.M. Young for their support and encouragement for this work. The technical support of J. Bryer, R.C. Cutler, H. Dymowski, E. Fredd, M.A. Goldman, M.P. McCarthy, and W. McCredie is also gratefully acknowledged.

This work was supported by U.S. DoE Contract No. DE-AC02-76-CHO-3073.

REFERENCES

[1] P.C. Efthimion, N.L. Bretz, M.G. Bell, M. Bitter, W.R. Blanchard, F.P. Boody, D.A. Boyd, C.E. Bush, J.L. Cecchi, J. Coonrod, S.L. Davis, D.L. Dimock, H.F. Dylla, S. von Goeler, R.J. Goldston, B. Grek, D.J. Grove, R.J. Hawryluk, H.W. Hendel, K.W. Hill, R. Hulse, D.W. Johnson, L.C. Johnson, R. Kaita, S.M. Kaye, M. Kikuchi, S.J. Kilpatrick, J. Kiraly, R. Knize, P.H. LaMarche, R. Little, D.M. Manos, M.P. McCarthy, D.C. McCune, K. McGuire, D.M. Meade, S.S. Medley, D.R. Mikkelsen, D. Mueller, M. Murakami, E.B. Nieschmidt, D.K. Owens, A.T. Ramsey, A.L. Roquemore, N.R. Sauthoff, J.F. Schivell, J-L. Schwob, S.D. Scott, S. Sesnic, J.C. Sinnis, F. Stauffer, J.D. Strachan, S. Suckewer, G.D. Tait, M. Tavernier, G. Taylor, F.H. Tenney, H.H. Towner, M. Ulrickson, K-L. Wong, A. Wouters, H. Yamada, K.M. Young, and M.C. Zarnstorff, Paper IAEA-CN-44/A-I-2 10th Intl. Conf. on Plasma Physics and Controlled Nuclear Fusion Research London, UK, (1984).

[2] R.J. Hawryluk, M.G. Bell, M. Bitter, W.R. Blanchard, N.L. Bretz, C.E. Bush, J.L. Cecchi, S.A. Cohen, J. Coonrod, S.L. Davis, D.L. Dimock, H.F. Dylla, P.C. Efthimion, R.J. Fonck, R.J. Goldston, S. von Goeler, B. Grek, D.J. Grove, H.W. Hendel, K.W. Hill, R.A. Hulse, J.A. Isaacson, D.W. Johnson, L.C. Johnson, R. Kaita, S.M. Kaye, S.J. Kilpatrick, J. Kiraly, R.J. Knize, R. Little, D.M. Manos, M.P. McCarthy, D.C. McCune, K. McGuire, D.M. Meade, S.S. Medley, D.R. Mikkelsen, D. Mueller, M. Murakami, E.B. Nieschmidt, D.K. Owens, A.T. Ramsey, A.L. Roquemore, N.R. Sauthoff, J.F. Schivell, S.D. Scott, S. Sesnic, J.C. Sinnis, P.C. Stangeby, J.D. Strachan, G.D. Tait, G. Taylor, F.H. Tenney, C.E. Thomas, J.R. Timberlake, H.H. Towner, M. Ulrickson, and K.M. Young,

Proceedings of the 4th Intl. Symp. on Heating in Toroidal Plasmas, Rome, Italy Vol. II, 1012, (1984).

[3] K.M. Young, M.G. Bell, W.R. Blanchard, N.L. Bretz, J.L. Cecchi, J. Coonrod, S.L. Davis, H.F. Dylla, P.C. Efthimion, R.J. Fonck, D.J. Grove, R.J. Hawryluk, H.W. Hendel, K.W. Hill, J. Isaacson, L.C. Johnson, R. Kalta, R.B. Krawchuk, R. Little, M.P. McCarthy, D.C. McCune, K. McGuire, D.M. Meade, S.S. Medley, D.R. Mikkelsen, D. Mueller, E.B. Nieschmidt, D.K. Owens, A.T. Ramsey, A.L. Roquemore, L.E. Samuelson, N.R. Sauthoff, J.F. Schivell, J.A. Schmidt, S. Sesnic, J.C. Sinnis, J.D. Strachan, G.D. Tait, G. Taylor, F.H. Tenney, and M. Ulrickson
Plasma Physics and Controlled Fusion 26, 11 (1984).

[4] V. Arunasalam, E.B. Meservey, M.M. Gurnee and R.C. Davidson, Phys. Fluids 11, 1076 (1968).

[5] A.E. Costley, R.J. Hastie, J.W.M. Paul, and J. Chamberlin, Phys. Rev. Lett 33, 758 (1974).

[6] V. Arunasalam, R. Cano and J.C. Hosea, Phys. Rev. Lett. 39, 408 (1977).

[7] P.C. Efthimion, V. Arunasalam and J.C. Hosea, Phys. Rev. Lett. 44, 396 (1980).

[8] P.C. Efthimion, V. Arunasalam, R. Bitzer, and J.C. Hosea, Temperature Vol. 5, Reinhold, NY (1982).

[9] G. Taylor, P.C. Efthimion, M.P. McCarthy, V. Arunasalam, R. Bitzer, J. Bryer, R.C. Cutler, E. Fredd, M.A. Goldman, and D. Kaufman, Rev. Sci. Inst. 55, 1739 (1984).

[10] F.W. Perkins, Proc. 3rd Intl. Symp. on Heating in Toroidal Plasmas, Rome, Italy Vol. II, 977, (1984).

[11] W.M. Tang, C.Z. Cheng, J.A. Krommes, W.W. Lee, C.R. Oberman, F.W. Perkins, G. Rewoldt, R. Smith, P. Bonoli, B. Coppi, R. Englade, J. Mastinelli, and L. Sugiyama, Paper IAEA-CN-44/E-III-8, 10th Intl. Conf. on Plasma Physics and Controlled Nuclear Fusion Research, London, UK, (1984).

[12] R.H. Dicke, Rev. Sci. Instrum. 17, 268 (1946).

[13] M.P. McCarthy, G. Taylor, P.C. Efthimion, E. Fredd, M.A. Goldman, R.C. Cutler, F.J. Stauffer, and D.A. Boyd, In Proc. of 8th Int. Conf. on Infrared and Millimeter Waves, Miami, Florida, paper m.4.5, (1983).

[14] W.H.M. Clark, Plasma Physics 25, 1501 (1983).

[15] D. Johnson, B. Grek, D. Dimock, D. Long, D. McNeill, D. Pallacino, J. Robinson, and E. Tolnas, Bull. Am. Phys. Soc. 23, 1383 (1984).

[16] B. Coppi, Comments Plasma Physics Cont. Fusion 5 261 (1980).

[17] H.P. Furth, P.H. Rutherford, and H. Solberg, Phys. Fluids 16, 1054 (1973).

[18] B.B. Kadomstev, Sov. J. Plasma Phys., 1, 389 (1975).

[19] A. Sykes and J.A. Wesson, Phys. Rev. Letters, 37, 140 (1976).

[20] G.L. Jahns, M. Soler, B.V. Waddell, J.D. Callen, and H.R. Hicks, Nucl. Fus. 18, 609 (1978).

[21] W. Pfeiffer, General Atomic, Report GA-A16994 (August 1983).

[22] W. Park and D. Monticello, Private Communication (1984).

[23] N.R. Sauthoff, K. McGuire, P.C. Efthimion, K.W. Hill, J. Kiraly, G. Taylor, and S. von Goeler, Bull. Am. Phys. Soc. 29, 1303 (1984).

[24] V.V. Parail and G.V. Pereverzev, Sov. J. Plasma Phys. 6, 14 (1980).

[25] K. McGuire and D.C. Robinson, Nucl. Fusion 19, 505 (1979).

[26] H. Yamada, K. McGuire, D. Colchin, P.C. Efthimion, E. Fredrickson, K.W. Hill, J. Kiraly, V. Pare, G. Taylor and N.R. Sauthoff, Princeton University, Plasma Physics Laboratory Report-2213 (1985).

[27] R.A. Jacobson,, C.E. Wagner and R.E. Covert, J. Fusion Energy 3, 217 (1983).

[28] F.J. Stauffer, D.A. Boyd, R.C. Cutler, and M.P. McCarthy, Rev. Sci. Instrum. 56, 925 (1985).

[29] E.B. Meservey, M. Bitter, C. Daughney, D. Eames, P.C. Efthimion, E. Hinnov, R. Hulse, D.A. Post, K. Sato, S. Suckewer, and S. von Goeler, Nucl. Fusion 24, 3 (1984).

[30] W. Pfeiffer and R.E. Waltz, Nucl. Fusion 19, 51 (1979).

[31] A. Gondhalekar R. Granetz, D. Gwinn, I. Hutchinson, B. Kusse, E. Marmar, D. Overskei, D. Pappas, R.R. Parker, M. Pickrell, J. Rice, L. Scaturro, J. Schuss, J. West, and S. Wolfe, Paper IAEA-CN-37/C-4, 7th Intl. Conference on Plasma Physics and Controlled Nuclear Fusion Research (Innsbruck, Austria, September 1978)

FIGURES

. Schematic of the TFTR heterodyne microwave radiometers. The radiometers were used to measure the fundamental ordinary mode and extraordinary mode second harmonic cyclotron emission on the horizontal midplane of the TFTR plasma.

2. Evolution of a 1.4 MA TFTR discharge with a minor radius of 0.83 m and an axial toroidal field of 2.7T. Surface voltage continues to fall during the current flattop.

3. Electron temperature profile evolution during the discharge shown in Fig. 2. At approximately one second into the discharge, temperature sawteeth break out at the center of the discharge and the profile broadens. Profiles were averaged for 100 msec to remove fluctuations on the profile due to the sawteeth.

4. Comparison of radiometer profile (solid curve) with laser Thomson scattering data (filled circles) during the current flattop of the same 1.4 MA TFTR discharge.

5. Broadening of the electron temperature profile with plasma current for B_T = 2.7 T and $\bar{n}_e$ = 2.1 - 2.3 x $10^{19} m^{-3}$. The q = 1 surface (indicated by arrows) grows as q_a is decreased from 4.7 to 2.5 while the temperature near the magnetic axis of the discharge remains very nearly constant.

6. Electron temperature profile dependence on $\bar{n}_e$ for I_p = 1.2 MA, B_T = 2.7 T and a = 0.83 m. Profile shape is insensitive to variation of $\bar{n}_e$. Profiles were averaged over 100 msec.

7. The electron temperature profile is shown for three plasmas with minor radii of 0.83, 0.69 and 0.55m. The arrows indicate the q = 1 surface. Profiles were averaged over 100 msec. The temperature normalized to the central temperature is independent of minor radius.

8. Time history of the central electron temperature for an I_p = 1.4 MA, a = 0.83 m and $\bar{n}_e$ = 3 x $10^{19} m^{-3}$ discharge. The filled circles are data determined from x-ray bremsstrahlung measured by a pulse height analyzer. The central electron temperature exhibits compound sawteeth at 2 to 3 seconds into the discharge.

9. Profile evolution during compound sawteeth in an I_p = 1.4 MA, a = 0.83 m, 2.7T plasma. The sudden collapse in central electron temperature is accompanied by a rise in temperature near the edge of the plasma.

10. The time history of a normal sawtooth fluctuation in the center of an I_p = 1.4 MA, B_T = 2.7 T, a = 0.83 m plasma is shown in the upper figure. The lower figure shows an overlay of electron temperature profiles at times before and after a full reconnection.

11. The time history of a compound sawtooth fluctuation in the center of a I_p = 1.4 MA, B_T = 2.7 T, a = 0.83 m plasma is shown in the upper figure. The two lower figures illustrate the change in temperature profile that occurs at a full reconnection (C and D) and a minor reconnection (A and B) away from the plasma axis.

12. (a) Visible bremsstrahlung Z_{eff} plotted against $\bar{n}_e$ for two density scans with I_p = 1.8 MA, B_T = 4.0T. The scans were taken on two days separated by six weeks so that the TFTR plasma had become cleaner for the later scan.

    (b) $T_{eo}/Z_{eff}^{0.5}$ plotted against $\bar{n}_e$ for the same density scans. When Z_{eff} dependence is removed the central temperature is independent of density for both density scans.

13. Central electron temperature plotted against the power scaling $B_T^{0.78}R^{-0.31}a^{1.1}Z_{eff}^{0.45}I_p^{-0.24}$ derived from regression of TFTR and PLT data. The TFTR data include B_T = 2.7 T (squares), 4 T (stars), 4.8 T (diamonds) deuterium, hydrogen and helium discharges with 0.5 < a < 0.83 m. Also plotted are TFTR a = 0.41 m deuterium discharges (triangles) where the central temperature was obtained from an absolutely calibrated Michelson Interferometer [28]. The PLT data include hydrogen and deuterium discharges with both carbon and stainless steel limiters (crosses).

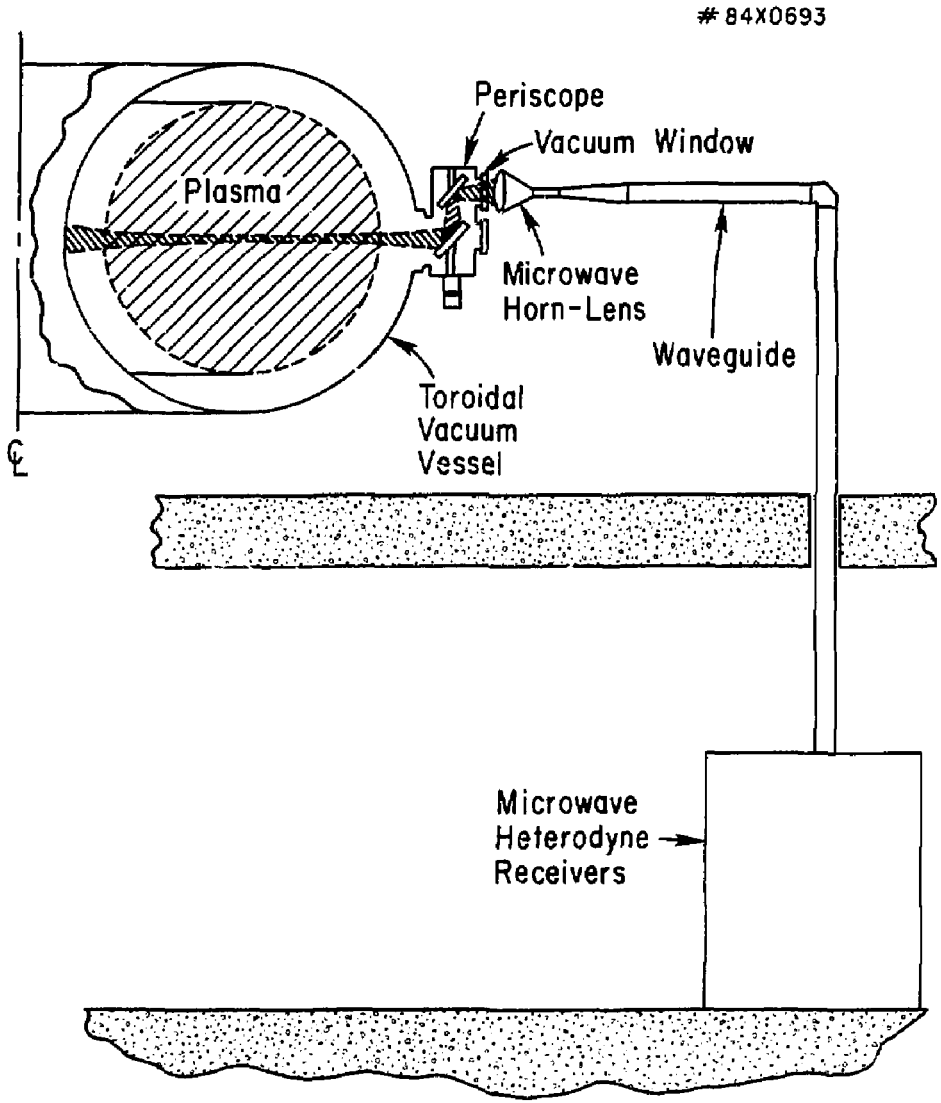
#84X0693
Periscope
Vacuum Window
Plasma
Microwave
Horn-Lens
Waveguide
Toroidal
Vacuum
Vessel
Microwave
Heterodyne
Receivers

Fig. 1

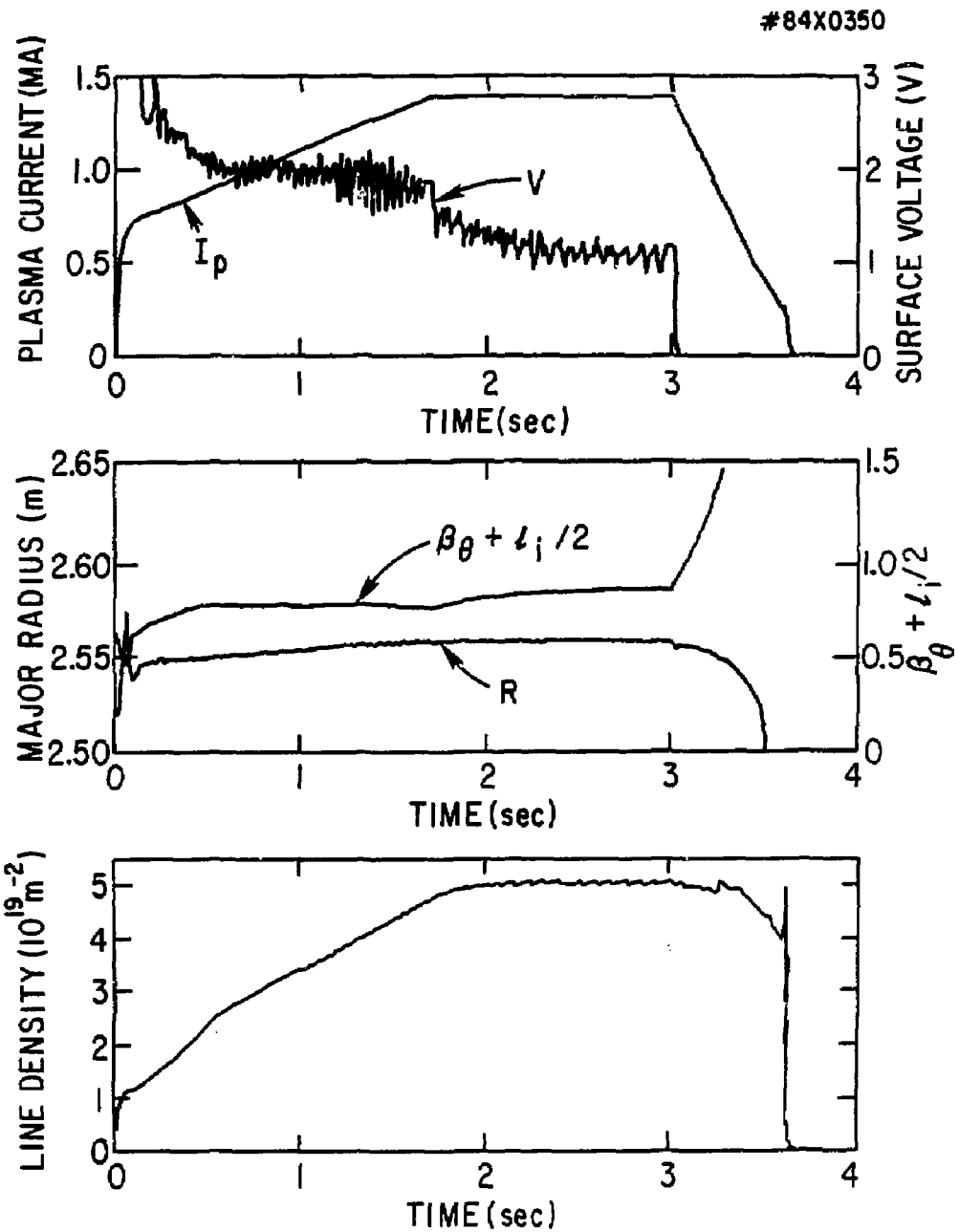
#84X0350
PLASMA CURRENT (MA)
SURFACE VOLTAGE (V)
I_p
V
TIME(sec)
MAJOR RADIUS (m)
$\beta_\theta + \ell_i/2$
R
TIME (sec)
LINE DENSITY (10^{19} m^{-2})
TIME (sec)

Fig. 2

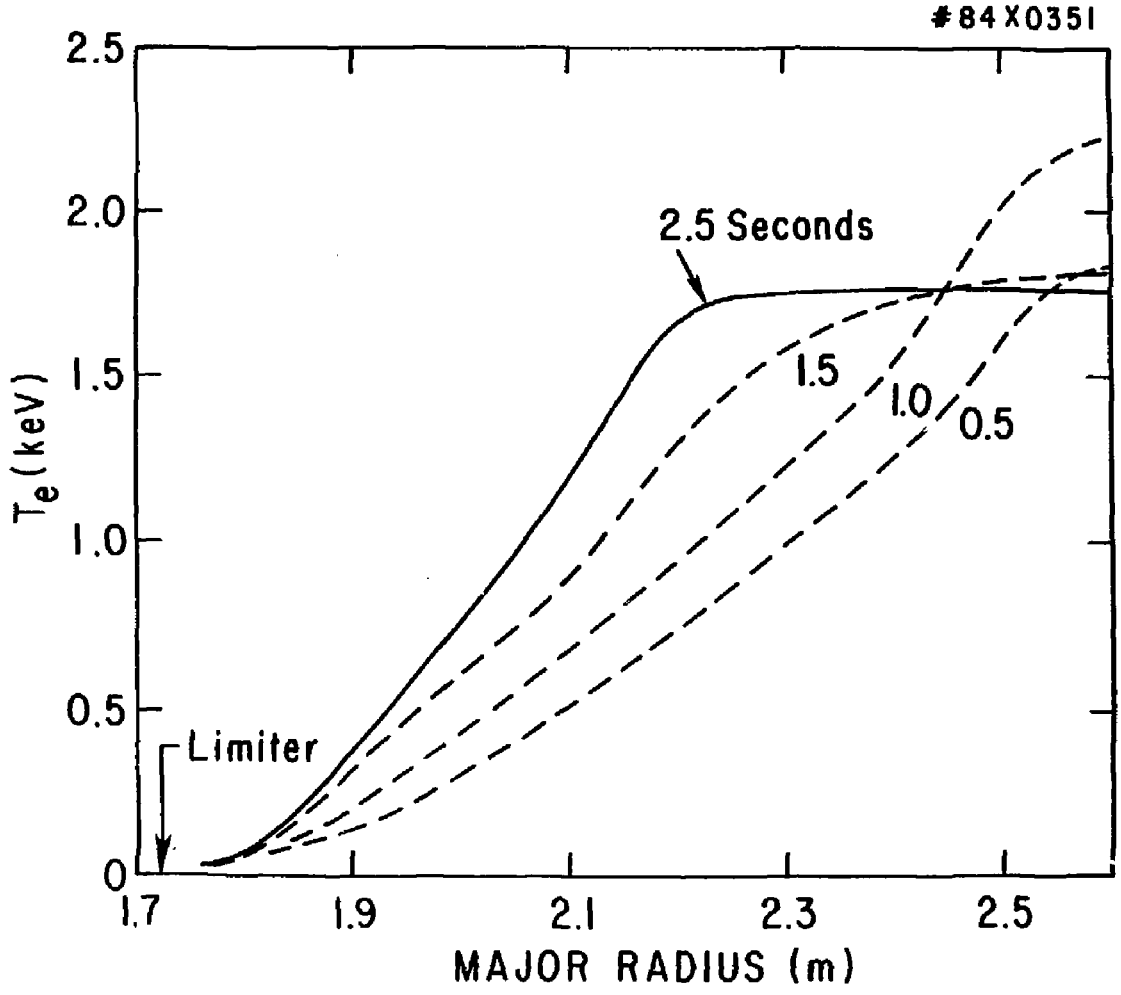
#84X0351
2.5
2.0
1.5
1.0
0.5
0
T_e (keV)
2.5 Seconds
1.5
1.0
0.5
Limiter
1.7
1.9
2.1
2.3
2.5
MAJOR RADIUS (m)

Fig. 3

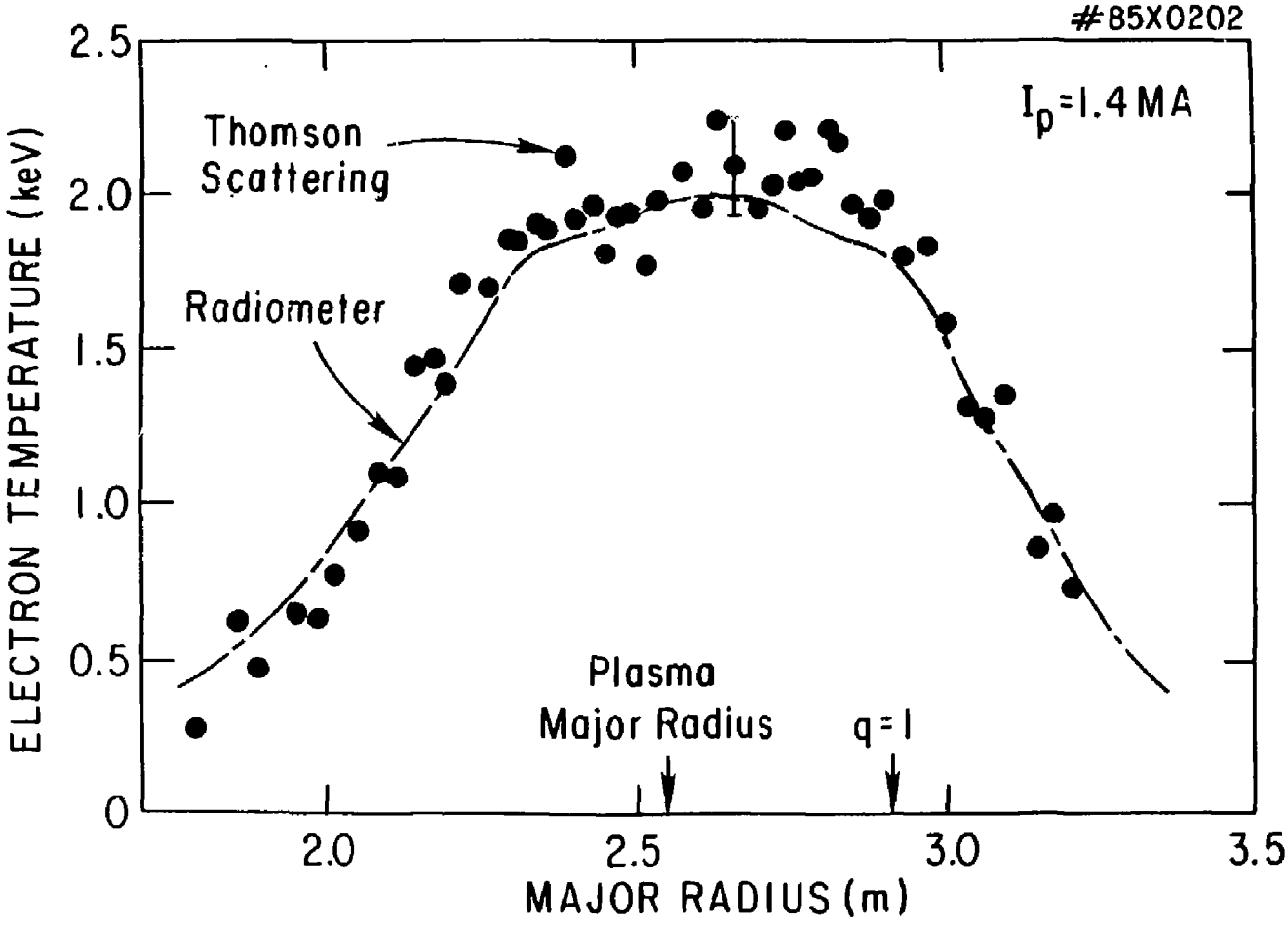
#85X0202
I_p=1.4 MA
Thomson Scattering
Radiometer
Plasma Major Radius
q=1
ELECTRON TEMPERATURE (keV)
MAJOR RADIUS (m)
0
0.5
1.0
1.5
2.0
2.5
2.0
2.5
3.0
3.5

Fig. 4

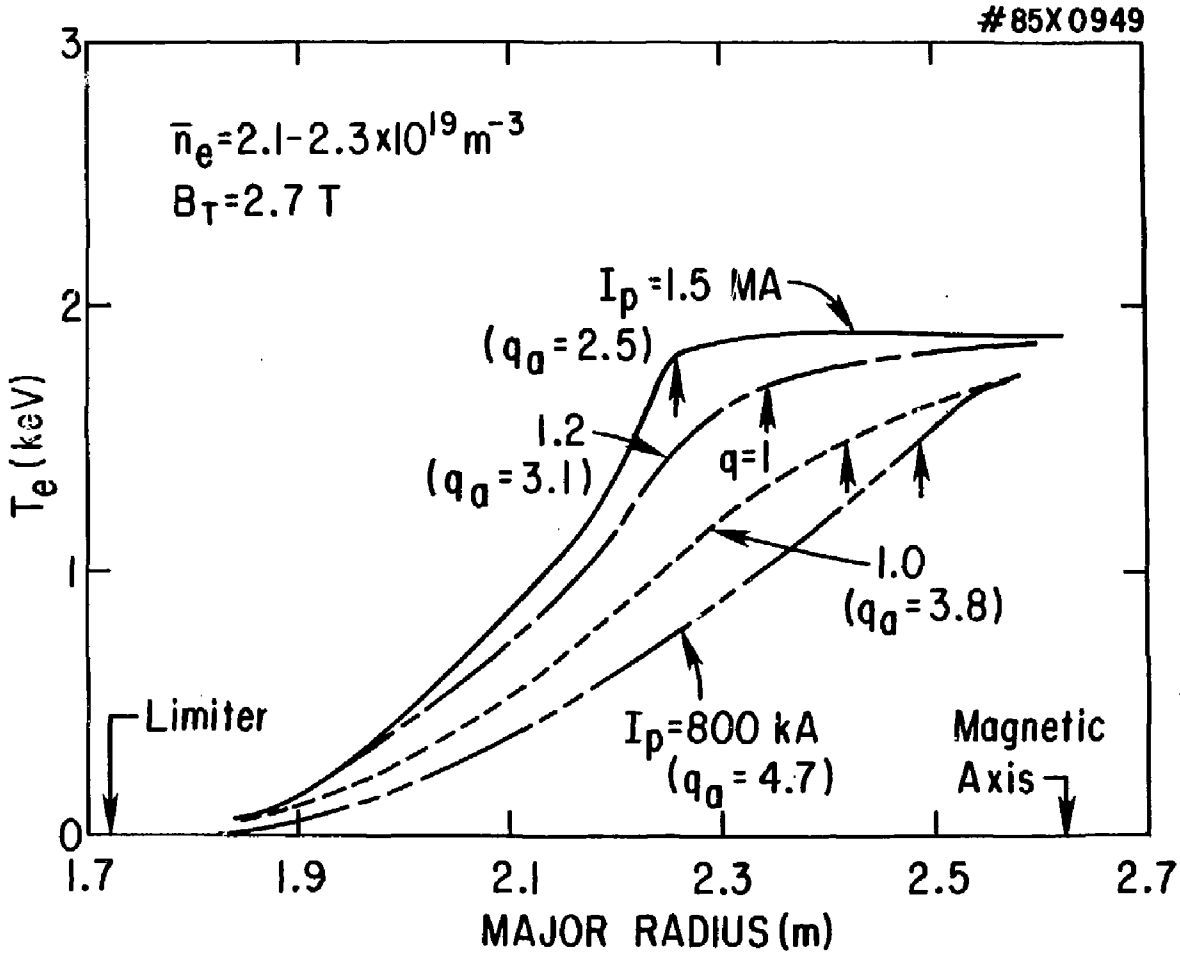
#85X0949
$\bar{n}_e$=2.1-2.3x10^{19}m^{-3}
B_T=2.7 T
I_p=1.5 MA
(q_a=2.5)
1.2
(q_a=3.1)
q=1
1.0
(q_a=3.8)
I_p=800 kA
(q_a=4.7)
Limiter
Magnetic Axis
T_e (keV)
MAJOR RADIUS (m)
0
1
2
3
1.7
1.9
2.1
2.3
2.5
2.7

Fig. 5

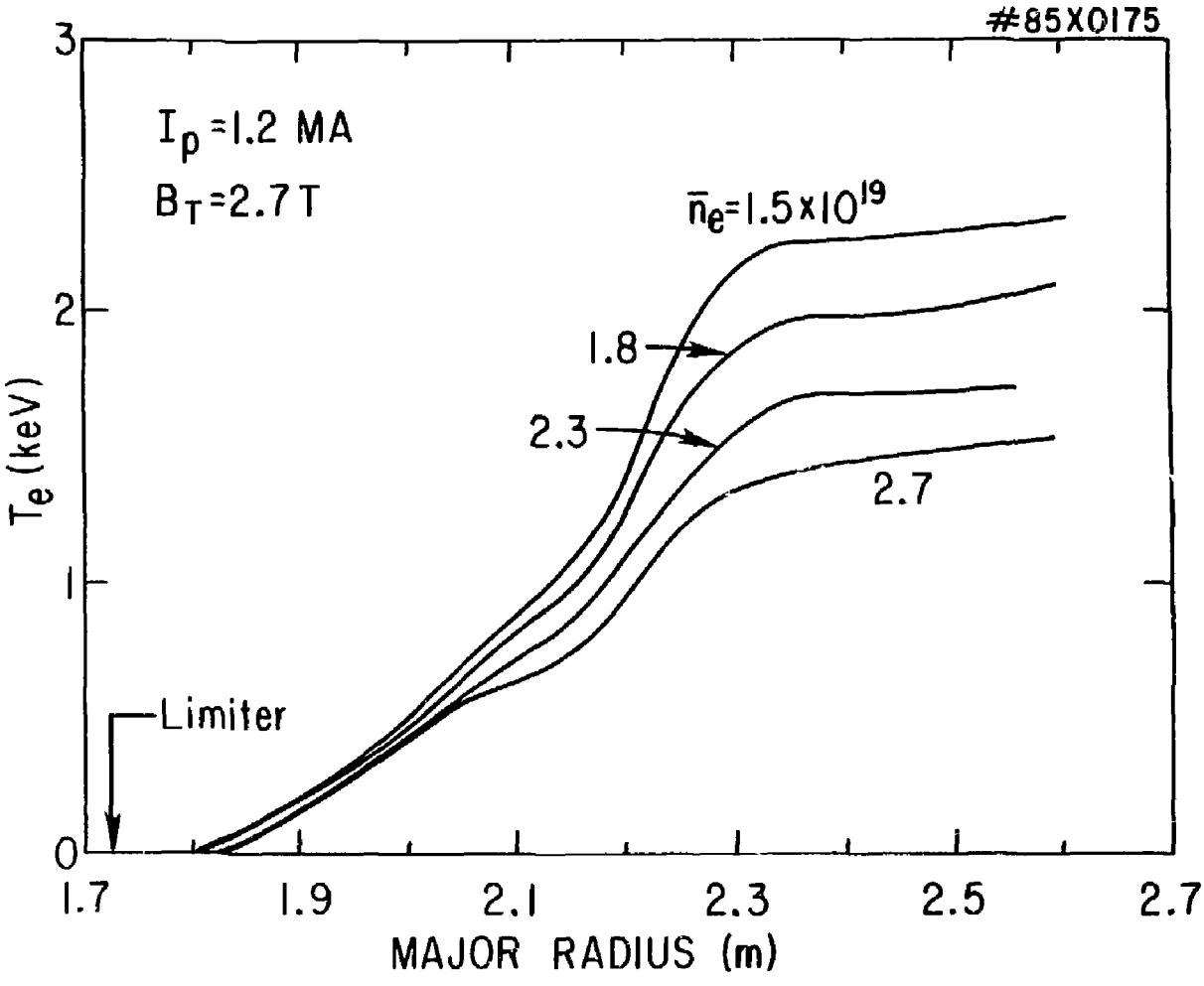
#85X0175
I_p = 1.2 MA
B_T = 2.7 T
$\bar{n}_e$ = 1.5 x 10^{19}
1.8
2.3
2.7
Limiter
T_e (keV)
MAJOR RADIUS (m)
0
1
2
3
1.7
1.9
2.1
2.3
2.5
2.7

Fig. 6

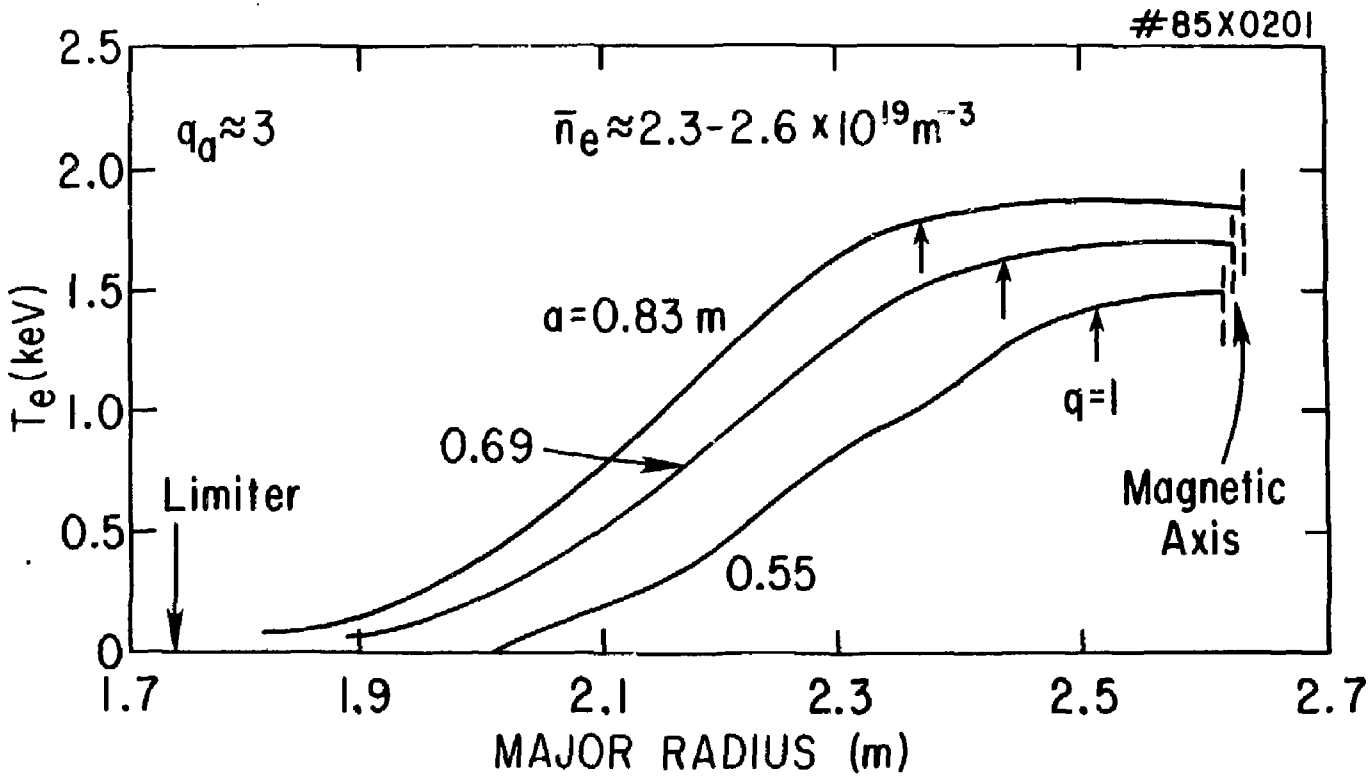
#85X0201
$q_a \approx 3$
$\bar{n}_e \approx 2.3\text{-}2.6 \times 10^{19} m^{-3}$
a=0.83 m
0.69
0.55
q=1
Limiter
Magnetic Axis
T_e (keV)
MAJOR RADIUS (m)
2.5
2.0
1.5
1.0
0.5
0
1.7
1.9
2.1
2.3
2.5
2.7

Fig. 7

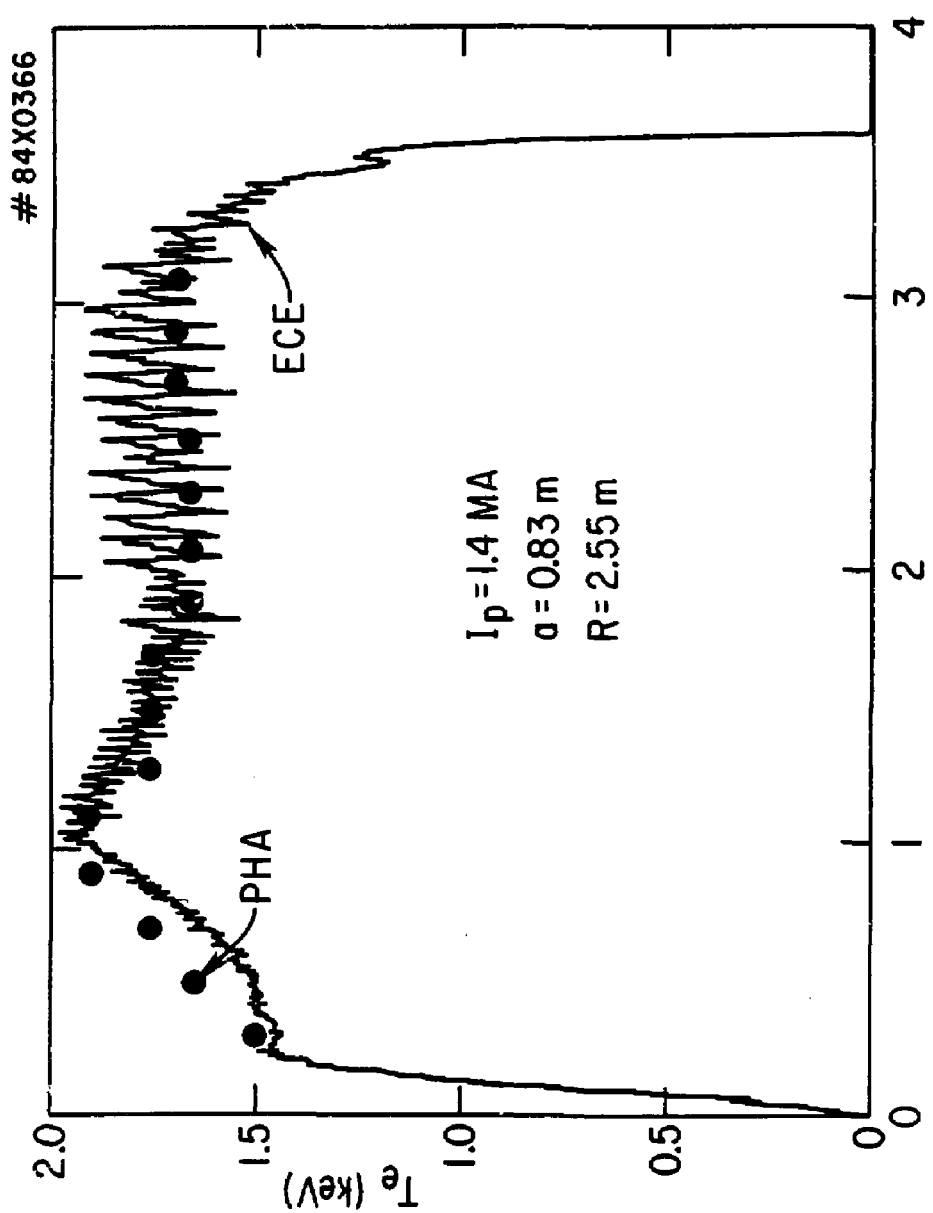
#84X0366
ECE
PHA
I_p=1.4 MA
a=0.83 m
R=2.55 m
T_e (keV)
TIME (sec)
2.0
1.5
1.0
0.5
0
1
2
3
4

Fig. 8

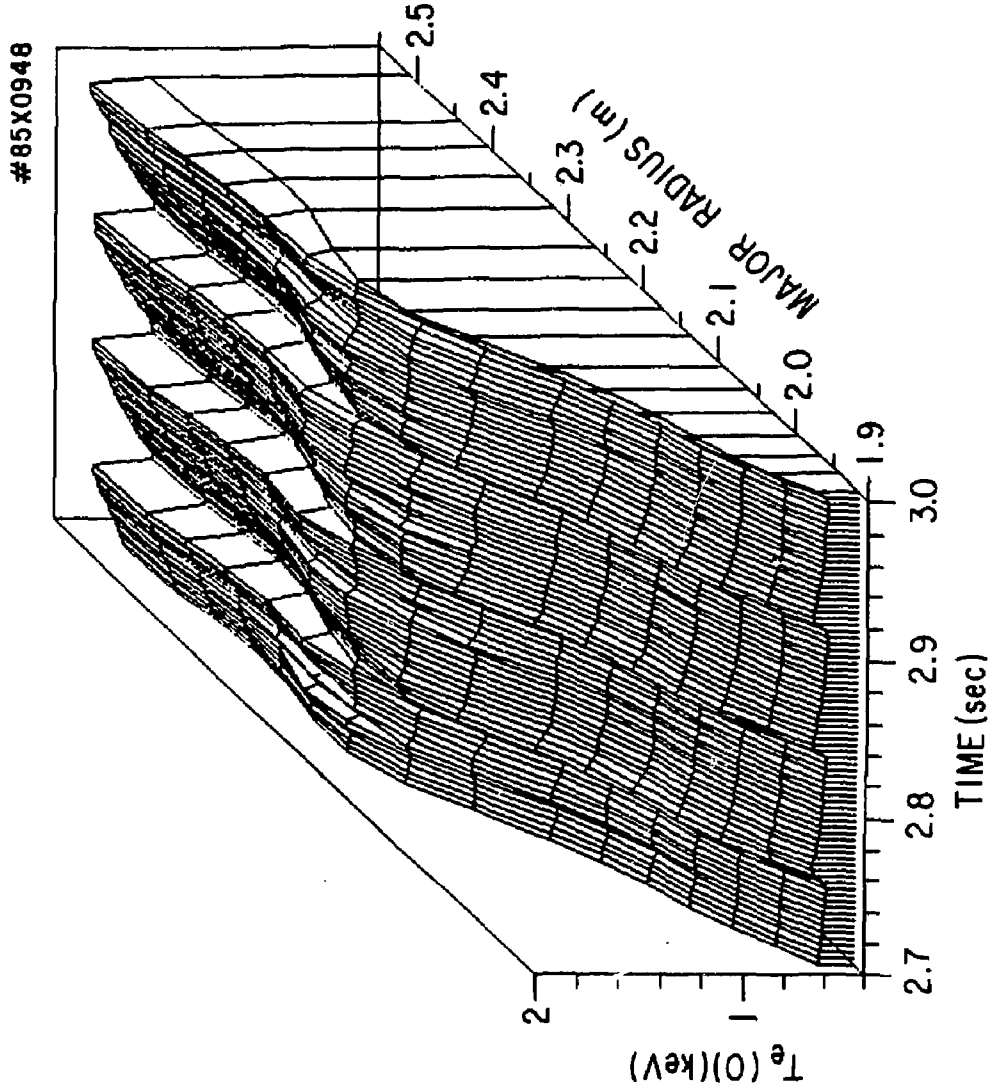
#85X0948
2.5
2.4
2.3
2.2
2.1
2.0
1.9
MAJOR RADIUS (m)
3.0
2.9
2.8
2.7
TIME (sec)
2
1
T_e (0) (keV)

Fig. 9

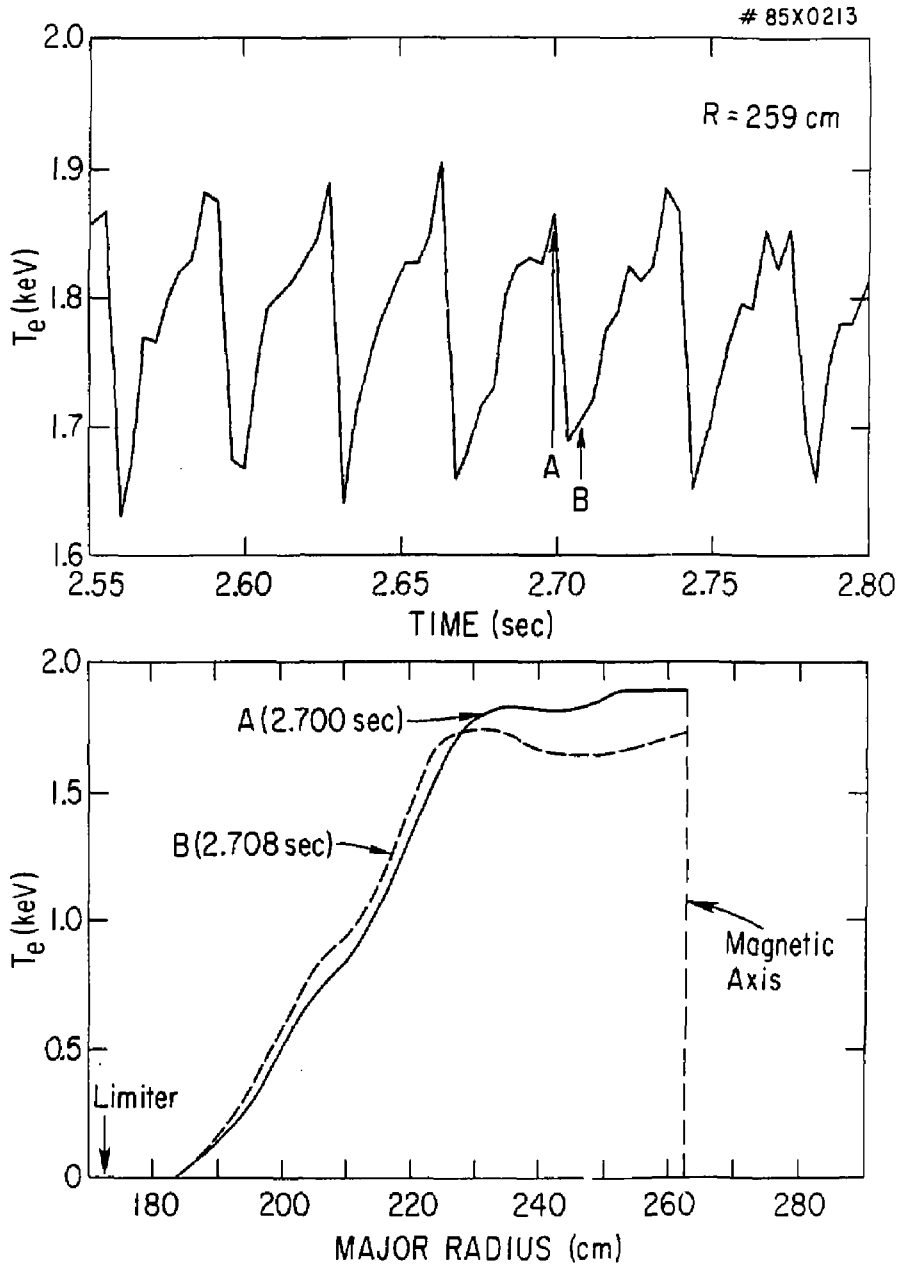
# 85X0213
R = 259 cm
T_e (keV)
TIME (sec)
A
B
A (2.700 sec)
B (2.708 sec)
Magnetic Axis
Limiter
MAJOR RADIUS (cm)

Fig. 10

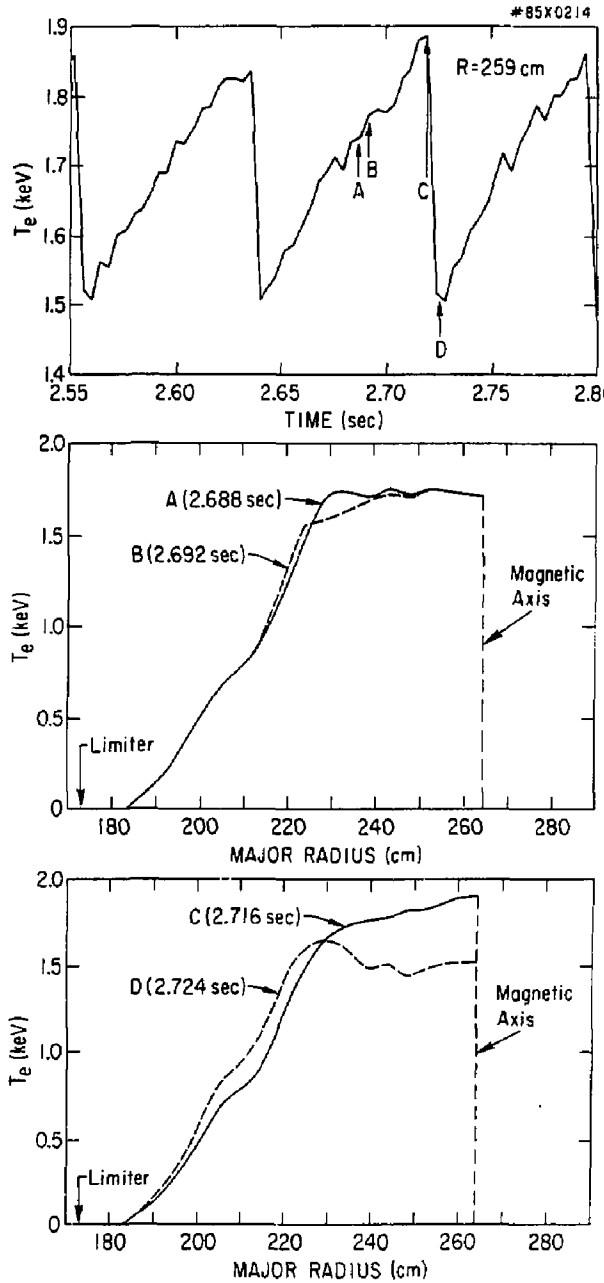
#85X0214
R=259 cm
A
B
C
D
T_e (keV)
TIME (sec)
A (2.688 sec)
B (2.692 sec)
Magnetic Axis
Limiter
MAJOR RADIUS (cm)
C (2.716 sec)
D (2.724 sec)
Magnetic Axis
Limiter
MAJOR RADIUS (cm)

Fig. 11

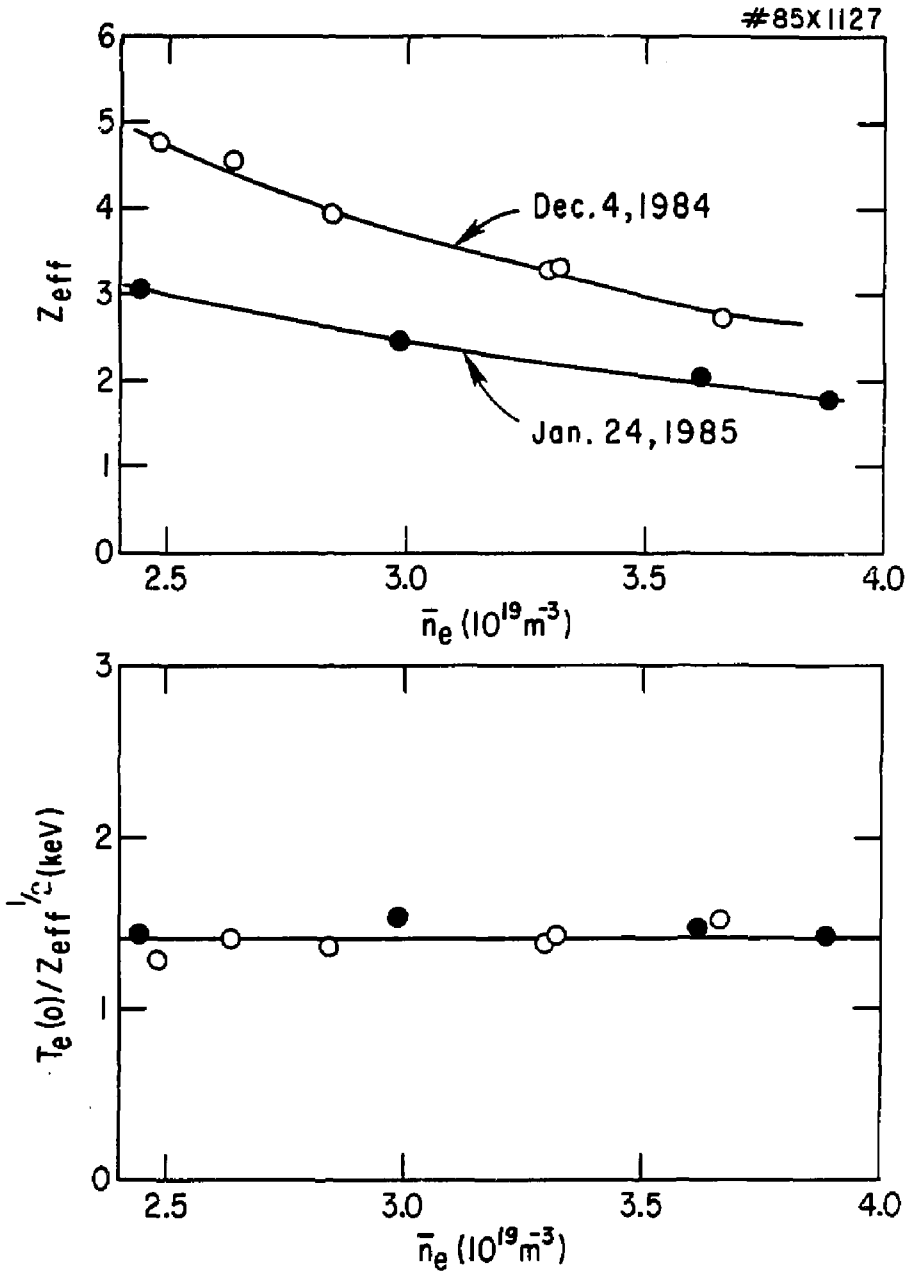
#85X1127
Dec. 4, 1984
Jan. 24, 1985
Z_{eff}
$\bar{n}_e$ (10^{19} m^{-3})
$T_e(0)/Z_{eff}^{1/2}$ (keV)
$\bar{n}_e$ (10^{19} m^{-3})

Fig. 12

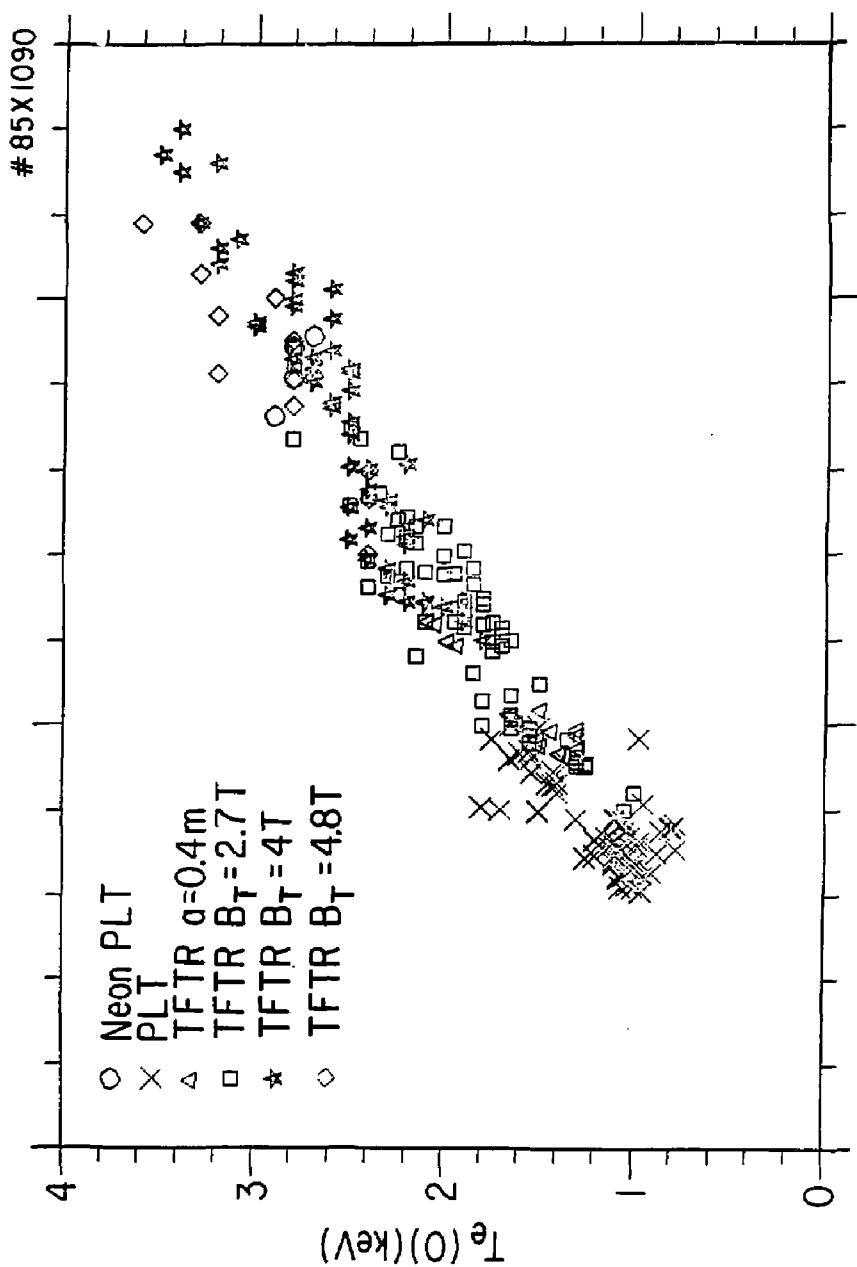
#85X1090
Neon PLT
PLT
TFTR a=0.4m
TFTR B_T=2.7T
TFTR B_T=4T
TFTR B_T=4.8T
$T_e(0)$(keV)
0
1
2
3
4
0
0.05
0.10
$B_T^{0.78}$ $Z_{eff}^{0.45}$ $a^{1.1}$ $R^{-0.31}$ $I_p^{-0.24}$

Fig. 13

EXTERNAL DISTRIBUTION IN ADDITION TO UC-20

Plasma Res Lab, Austra Nat'l Univ, AUSTRALIA
Dr. Frank J. Paoloni, Univ of Wollongong, AUSTRALIA
Prof. I.R. Jones, Flinders Univ., AUSTRALIA
Prof. M.H. Brennan, Univ Sydney, AUSTRALIA
Prof. F. Cap, Inst Theo Phys, AUSTRIA
Prof. Frank Verheest, Inst theoretische, BELGIUM
Dr. D. Palumbo, Dg XII Fusion Prog, BELGIUM
Ecole Royale Militaire, Lab de Phys Plasmas, BELGIUM
Dr. P.H. Sakanaka, Univ Estadual, BRAZIL
Dr. C.R. James, Univ of Alberta, CANADA
Prof. J. Teichmann, Univ of Montreal, CANADA
Dr. H.M. Skarsgard, Univ of Saskatchewan, CANADA
Prof. S.R. Sreenivasan, University of Calgary, CANADA
Prof. Trevor W. Johnston, INRS-Energie, CANADA
Dr. Hannes Barnard, Univ British Columbia, CANADA
Dr. M.P. Bachynski, MPB Technologies, Inc., CANADA
Chalk River, Nucl Lab, CANADA
Zhengwu Li, SW Inst Physics, CHINA
Library, Tsing Hua University, CHINA
Librarian, Institute of Physics, CHINA
Inst Plasma Phys, Academia Sinica, CHINA
Dr. Peter Lukac, Komenskeho Univ, CZECHOSLOVAKIA
The Librarian, Culham Laboratory, ENGLAND
Prof. Schatzman, Observatoire de Nice, FRANCE
J. Radet, CEN-BP6, FRANCE
AM Dupas Library, AM Dupas Library, FRANCE
Dr. Tom Mual, Academy Bibliographic, HONG KONG
Preprint Library, Cent Res Inst Phys, HUNGARY
Dr. S.K. Trehan, Panjab University, INDIA
Dr. Indra Mohan Lal Das, Banaras Hindu Univ, INDIA
Dr. L.K. Chavda, South Gujarat Univ, INDIA
Dr. R.K. Chhajlani, Vikram Univ. INDIA
Dr. B. Dasgupta, Saha Inst, INDIA
Dr. P. Kaw, Physical Research Lab, INDIA
Dr. Phillip Rosenau, Israel Inst Tech, ISRAEL
Prof. S. Cuperman, Tel Aviv University, ISRAEL
Prof. G. Rostagni, Univ Di Padova, ITALY
Librarian, Int'l Ctr Theo Phys, ITALY
Miss Clelia De Palo, Assoc EURATOM-ENEA, ITALY
Biblioteca, del CNR EURATOM, ITALY
Dr. H. Yamato, Toshiba Res & Dev, JAPAN
Direc. Dept. Lg. Tokamak Dev. JAERI, JAPAN
Prof. Nobuyuki Inoue, University of Tokyo, JAPAN
Research Info Center, Nagoya University, JAPAN
Prof. Kyoji Nishikawa, Univ of Hiroshima, JAPAN
Prof. Sigeru Mori, JAERI, JAPAN
Library, Kyoto University, JAPAN
Prof. Ichiro Kawakami, Nihon Univ, JAPAN
Prof. Satoshi Itoh, Kyushu University, JAPAN
Dr. D.I. Choi, Adv. Inst Sci & Tech, KOREA
Tech Info Division, KAERI, KOREA
Bibliotheek, Fom-Inst Voor Plasma, NETHERLANDS
Prof. B.S. Liley, University of Waikato, NEW ZEALAND
Prof. J.A.C. Cabral, Inst Superior Tecn, PORTUGAL
Dr. Octavian Petrus, ALI CUZA University, ROMANIA
Prof. M.A. Hellberg, University of Natal, SO AFRICA
Dr. Johan de Villiers, Plasma Physics, Nucor, SO AFRICA
Fusion Div. Library, JEN, SPAIN
Prof. Hans Wilhelmson, Chalmers Univ Tech, SWEDEN
Dr. Lennart Stenflo, University of UMEA, SWEDEN
Library, Royal Inst Tech, SWEDEN
Centre de Recherchesen, Ecole Polytech Fed, SWITZERLAND
Dr. V.T. Tolok, Kharkov Phys Tech Ins, USSR
Dr. D.D. Ryutov, Siberian Acad Sci, USSR
Dr. G.A. Eliseev, Kurchatov Institute, USSR
Dr. V.A. Glukhikh, Inst Electro-Physical, USSR
Institute Gen. Physics, USSR
Prof. T.J.M. Boyd, Univ College N Wales, WALES
Dr. K. Schindler, Ruhr Universitat, W. GERMANY
Nuclear Res Estab, Julich Ltd, W. GERMANY
Librarian, Max-Planck Institut, W. GERMANY
Bibliothek, Inst Plasmaforschung, W. GERMANY
Prof. R.K. Janev, Inst Phys, YUGOSLAVIA